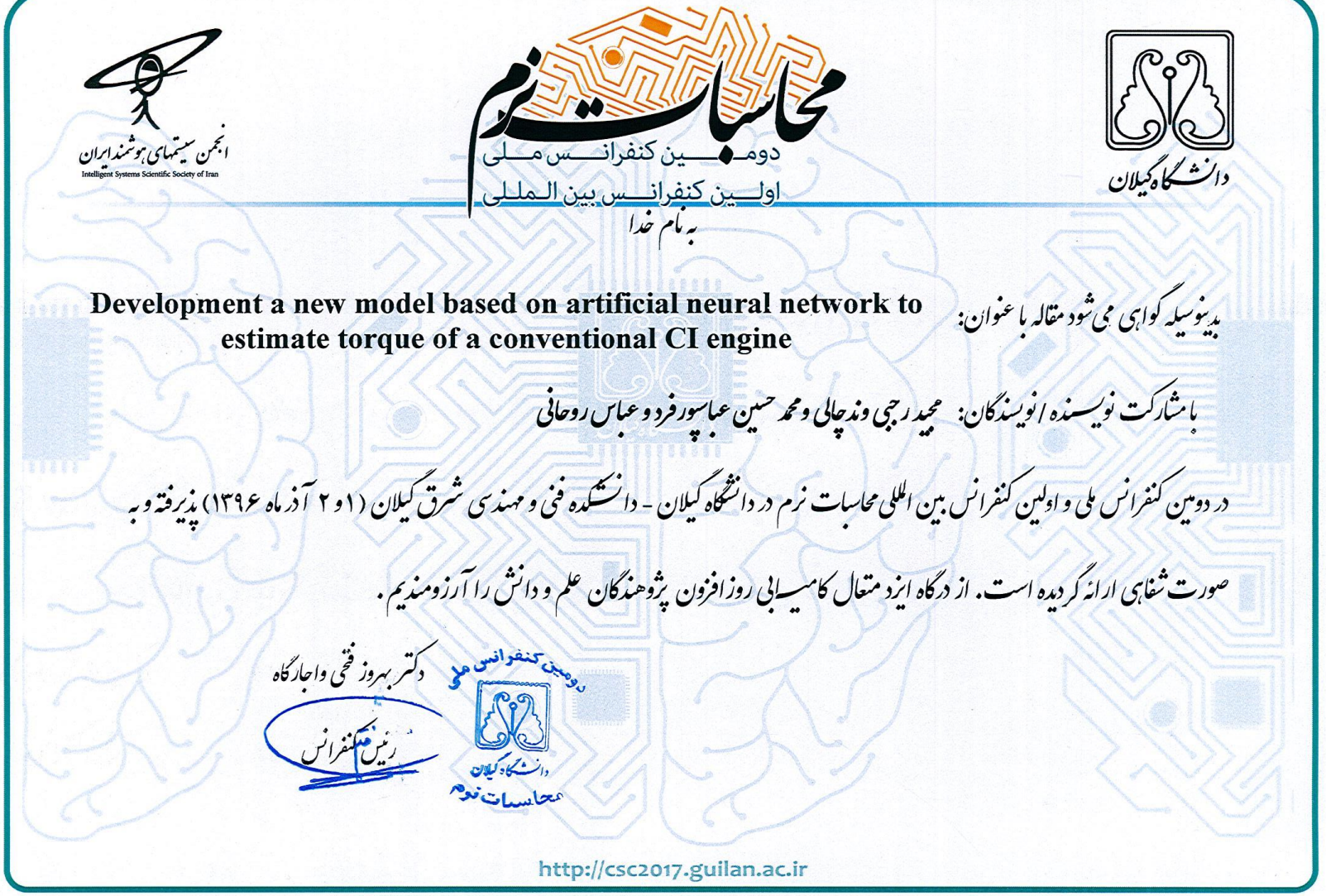

University of Guilan
2nd National Conference on Soft Computing
Intelligent systems Scientific Society of Iran

Development a new model based on artificial neural network to estimate torque of a conventional CI engine

Majid Rajabi Vandechali[1*], Mohammad Hossein Abbaspour-Fard[2], Abbas Rohani[3]

1- PhD student, Department of Biosystems Engineering, Faculty of Agriculture, Ferdowsi University of Mashhad, Mashhad, Iran.

2- Professor, Department of Biosystems Engineering, Faculty of Agriculture, Ferdowsi University of Mashhad, Mashhad, Iran. E-mail: abaspour@um.ac.ir

3- Assistant Professor, Department of Biosystems Engineering, Faculty of Agriculture, Ferdowsi University of Mashhad, Mashhad, Iran. E-mail: arohani@um.ac.ir

* Corresponding Author: m_rajabivandechali@stu.um.ac.ir

Abstract

Torque estimation needs intensive efforts and costly sensors. In this research, a model was proposed to estimate ITM285 tractor engine torque using some low cost sensors. Radial basis function (RBF) neural network was used for torque estimation, based on the data obtained from some inexpensive sensors including engine speed, exhaust gas opacity, fuel mass flow and exhaust gas temperature. Thirteen training algorithms were examined to train the RBF. These algorithms were compared using two statistical methods namely k-fold cross validation and completely randomized design (CRD). The Bayesian regularization (Trainbr) algorithm was the best one. Based on the sensitivity analysis of the RBF, only using engine speed, fuel mass flow and exhaust gas temperature sensors are sufficient for proper engine torque estimation. R^2, RMSE and EF of the RBF were 0.99, 0.50 and 0.99, respectively. It is concluded that the RBF model can be a suitable technique for estimating engine torque.

Keywords: Engine torque, Low cost sensor, Neural network, Sensitivity analysis, Training algorithm.

1. INTRODUCTION

Nowadays diesel engine is the heart of a wide range of machines and equipment especially tractors, so keeping it in a good working condition is vital for a good overall efficiency [1]. Most of agricultural implements are powered by power-take-off (PTO) shaft of tractor. On the go estimation of rotary power consumption of these implements is very important for farm power management purpose. Monitoring tractor engine torque is crucial

for engineers to design and for farm experts to manage and to make proper decision. Furthermore, accurate measurement of the engine rotary load is time intensive and costly. Hence, condition monitoring (CM) of transmitted torque and power of tractor engine can be beneficial for control system applications. These are the motivations of this research.

Most of former researches on torque estimation have focused on internal combustion (IC) engine models. The inputs of these models typically consist some engine measurements such as air [2] or fuel [3] mass flow, throttle position [4, 5], fuel properties [6], spark advance [2, 5], engine speed [2, 3, 5, 6], acoustic emission features [7], etc. Lee et al. [8] introduced two torque estimation techniques, namely "Stochastic Estimation Technique" and "Frequency Analysis Technique", for an in-line, four-cylinder SI engine under a wide range of engine operating conditions (different engine speeds and loads). Lin et al. [9] have employed instantaneous crank angular speed (IAS) as a non-intrusive CM technique to estimate the load on a four-stroke, four-cylinder diesel engine in a laboratory condition. Numerous static and dynamic torque estimation methods were presented to monitor the engine torque [4]. Through a research work four statistical methods were reviewed in a unified framework and compared for building the torque model: linear least squares, linear neural networks (NNs), non-linear NNs and support vector machines (SVM). It was concluded that a non-linear model structure is essential for accurate torque estimation [10].

Using artificial neural networks (ANNs) to improve torque estimation of IC engines has become increasingly widespread [11]. Tosun et al. [6] used ANN based on back-propagation Levenberg-Marquardt (BPLM) training algorithm and linear regression (LR) modeling to predict engine torque and some other engine performance parameters of a diesel engine. They mentioned that experimental determination of performance and emission characteristics of an IC engine is complex, costly and time consuming. Therefore, the engine performance parameters were modeled using ANN in order to eliminate these disadvantages and complexities. They used some parameters including exhaust temperature, fuel consumption and engine vibration as inputs and the models were presented for different fuel types, separately. The performance comparison of LR and ANN showed that more accurate results can be obtained for the predicted parameters with ANN technique. Ge et al. [11] categorized the torque estimation models in two groups: in one category, the engine is modeled in detail according to physical mechanism of engine, and then the engine torque is estimated using the detailed model, e.g. [12]; in the other category, the complex nonlinear physical process of the detailed model is identified by using an ANN, resulting in a simplified model, and then the torque is estimated using the simplified model. Other prediction works related to the engine torque of IC engines based on ANN approach were presented elsewhere, e.g. [13, 14].

The applications of RBF networks for modeling engine torque are rare. The prime benefit of using RBF feed-forward neural networks is less required training time which is due to simpler structure of these ANNs compared to the other networks. RBF also has comparatively low extrapolation errors and is generally more reliable [15]. Therefore, in the present study, the ability of RBF neural network with various training algorithms was investigated to predict the CI engine torque under various working conditions, and their performances were compared. This is done with the aim of improving the accuracy of torque estimation.

In conclusion, the engine torque is one of the most important performance parameters of IC engines, which frequently needs to be estimated during operations. However its accurate measuring is laborious, time-consuming and costly. ITM285 is the most common tractor in Iran that is widely used in agricultural operations. Accurate estimation of the output engine torque exerted by active agricultural implements through the PTO shaft of tractor can be used for instantaneous system management during field operations. This is an important and effective aspect of precision farming which is developing in the current century. Hence, the main objective of this study was to develop engine torque estimation models in a wide range of engine operating conditions (load and speed) based on soft computing methods. The specific objectives were: 1- to investigate the effectiveness of RBF neural network for engine torque estimation; 2- to study the variation of model performance with different model parameters; 3- to select the most appropriate model for accurate prediction of engine torque.

2. MATERIALS AND METHODS

2.1. ENGINE CHARACTERISTICS

Currently ITM285 tractor is the most popular tractor in Iran. It was adopted with different weather conditions of country and hence most of agricultural operations are performed by this model [16]. An ITM285 tractor was employed and the experiments were performed at the Department of Biosystems Engineering, College of Agriculture, Ferdowsi University of Mashhad, Iran. The detailed characteristics of the tractor's engine are shown in Table 1. Before commencing the experiments, all filters of the fuel and lubrication systems were renewed. Some preliminarily tests were conducted to verify the instruments and to ensure the proper status of the engine for the main tests [17].

Table 1- Characteristics of the tractor's engine.

Engine type	Perkins, four-cylinder, four-stroke, CI
Model year (MY)	2005
Cylinder bore	101 mm
Cylinder stroke	127 mm
Compression ratio	16:1
Fuel	Diesel fuel
Fuel pump	in-line injection pump
Combustion system	Direct injection
Maximum power	75 hp @ engine speed of 2000 rpm
PTO RPM	540 rpm @ engine speed of 1818 rpm

2.2. EXPERIMENTAL PROCEDURES

Experiments were conducted at 11 levels of primary engine speed (PES) including: 779, 923, 1063, 1204, 1346, 1488, 1629, 1771, 1818 (engine rated speed), 1913 and 2054 rpm (from 935 to 2465 rpm of the dynamometer speed by steps of 170 rpm). The tractor's PTO was coupled to a hydraulic dynamometer through a universal joint. At the beginning of each test, the engine speed was set and fixed at the desired level, using the hand throttle lever of tractor and the engine was sufficiently warmed up [18]. In other words, the engine hand throttle position was kept fixed while exerting the load. In each PES, the applied torque on the engine started from zero (no load) and continued to full load by increment of 10 N.m. As expected, the engine speed continuously decreased with increasing the applied torque. Hence, the engine speed at zero load and during experiment (corresponding to the applied torque) were named PES and instantaneous engine speed (IES), respectively. The overall view of the test setup is shown in Figure 1. The measured parameters include fuel consumption mass flow (FCMF), exhaust gas temperature (EGT), IES, maximum exhaust opacity (MAEO) and mean exhaust opacity (MEEO). The experiments were carried out at ambient temperature range of 23 ± 7 °C [19].

Figure 1. The overall view of the test setup.

2.3. MEASURING PARAMETERS

A hydraulic water-flow dynamometer (PLINT, England) with maximum loading capacity of 325 N.m was used to exert rotational load on the engine, via PTO shaft (Figure 1). The instrumentations for measuring parameters and the schematic of the test bed are shown in Figure 2 and Figure 3, respectively. Data recording was performed after achieving stability in values of instrumentations at each new torque or speed points [17]. To measure the torque applied on the engine by the dynamometer, it was equipped with a load cell with capacity of 100 kg. The load cell output is sent to a personal computer (PC) and is then converted to torque unit by multiplying with torque arm (0.365 m). Prior to starting the experiments, the dynamometer was statically calibrated using the existing standard weights (two weights correspond to 50 N.m and two weights of 75 N.m). Also, the rotational measuring component of the dynamometer was calibrated using an optical tachometer. The readings of dynamometer for RPM and torque were received by an electronic interface circuit and were digitally sent to the PC and then, were displayed on a monitor. The conversion ratio of engine speed to dynamometer speed was 1:1.2. In other words, the engine speed was calculated by dividing the dynamometer speed to 1.2. For precise adjustment of a PES at an intended level, the tractor's hand throttle was disconnected from injection pump and replaced with a suitable scaled screw on control rack lever of the injection pump.

Fuel consumption (by mass) was accurately determined by means of a digital scale through weighing the weight of a temporary small fuel supply container (instead of tractor's main fuel tank). The volumetric measurement of fuel consumption is much easier than the mess measurement but temperature corrections must be applied [17]. When consumption is measured by volume, the fuel density at 15 °C should be multiplied by the fuel temperature at which the measurement was made [19]. Hence, the fuel density variations with temperature must

be considered. A digital scale (Japan, A&D Co., 6 kg capacity, ±0.01 g) was used to measure FCMF of the engine (Figure 2). The tractor's fuel tank was disconnected from fuel system and instead a small fuel container was used and carefully put on the scale. The fuel flow from container is conveyed to primary fuel filters through a plastic pipe and another pipe was used to return the surplus fuel from injectors to the container (Figure 3). The weight of container on the scale was recorded with sampling rate of five samples per second. Afterwards, the scatter plot of the recorded values was drawn by Excel software and then the trend line of the plot is fitted. The FCMF is determined in gram per second which is corresponds to the slop of the trend line.

A diesel emission tester (Germany, MAHA Co., MDO2-LON model) was used to measure exhaust opacity (Figure 2). Before starting the experiments, the device was calibrated by the authorized company (Iran, Tavan Sazan Co.). This device measures and records the exhaust opacity in m^{-1}, and displays the variations of MAEO at the end of each test run.

Figure 2. The instrumentations for measuring the parameters: 1- Digital scale to measure fuel consumption, 2- Diesel emission tester, 3- Temperature monitor and sensor, 4- Emission probe and 5- Load cell.

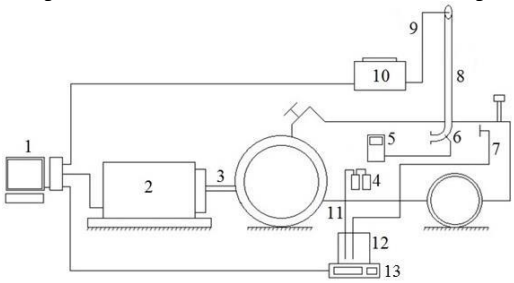

Figure 3. Schematic of the test bed: 1- Data acquisition system, 2- Dynamometer, 3- Universal joint, 4- Primary fuel filters, 5- Temperature monitor, 6- Temperature sensor, 7- Fuel return pipe, 8- Tractor exhaust, 9- Emission measurement probe, 10- Diesel emission tester, 11- Fuel inlet pipe, 12- Fuel container and 13- Digital scale.

A K-type temperature sensor (thermocouple) capable of measuring temperature up to 700 ºC [20] was installed on the exhaust elbow [21] and a temperature monitor (Lutron Co., TM-902C model, capable of monitoring temperature from -50 to 1300 ºC, resolution of 1 ºC) were used (Figure 2). The accuracy of the temperature sensor was examined by measuring the temperatures of saturated mixture of water and ice (0 ºC) and boiling water (99.62 ºC) at atmospheric pressure of 100 kPa [22]. The exhaust elbow was drilled to install the temperature sensor on the engine [21] and a hexagon nut was weld on the drilled hole. The sensor completely entered into the elbow by tightening the sensor base to the nut (Figure 2). The exhaust elbow was selected to install the temperature sensor for two reasons: 1- all exhaust gases of cylinders pass through this component, and 2- this component is the nearest place to the exhaust manifold and hence minimum reduction of exhaust gas temperature occurs. Precisely speaking, the midpoint of elbow curvature was considered as installation location of the sensor, where the exhaust gases pass tangentially to the internal wall and hence better affect the temperature sensor (Figure 3).

2.4. DATA ANALYSIS

In the present study, RBF neural network model was employed to estimate the engine output torque. RBF is a kind of learning algorithm method of ANNs, which offers faster prediction than a conventional simulation program or mathematical technique [23]. A RBF-based ANN structure includes three layers named input, hidden, and output layers [24]. The hidden layer consists of many RBF neurons and its nodes are calculated from the Euclidean distance between the center and the network input vectors [25]. The RBF neural network offers more effective methods to train and organize its structure and does not have the problem of trapping into the local minimum [26]. It is one of the variants of feed-forward ANN types. Such ANNs are applied to execute mapping functions of the form $f: \mathcal{R}^n \rightarrow \mathcal{R}$ based on the following equation:

$$f(x) = W_0 + \sum_{i=0}^{m} W_i \, \varphi(\|x - c_i\|) \quad (1)$$

where $x \in \mathcal{R}^n$ represents the input vector, $\varphi(.)$ is a non-linear transformation function, $\|.\|$ represents the Euclidean distance, W_i having a range of $1 \leq i \leq m$ represents the weights, $c_i \in \mathcal{R}^n$ having a range of $1 \leq i \leq m$ denotes the kernel nodes or centers, with m representing the number of kernel nodes. A radial basis function network based on Eq. 1 which is adopted for the inputs and output of this study is shown in Figure 4 [15].

Thirteen training algorithms including Bayesian regularization (Trainbr), BFGS quasi-Newton back-propagation (Trainbfg), Powell-Beale conjugate gradient back-propagation (Traincgb), scaled conjugate gradient back-propagation (Trainscg), Fletcher-Powell conjugate gradient backpropagation (Traincgf), one step secant back-propagation (Trainoss), Polak-Ribiere conjugate gradient back-propagation (Traincgp), Levenberg-Marquardt back-propagation (Trainlm), resilient back-propagation (Trainrp), gradient descent w/momentum and adaptive lr back-propagation (Traingdx), gradient descent with adaptive lr back-propagation (Traingda), gradient descent with momentum back-propagation (Traingdm) and gradient descent back-propagation (Traingd) were used to examine their effectiveness in training the RBF neural network. Kumar et al. [27] used four different training algorithms (Trainrp, Traingdx, Trainscg and Trainlm) for training the network. The training algorithms were compared together using the combination of three statistical methods namely: k-fold cross validation [28], completely randomized design (CRD) and least significant difference (LSD).

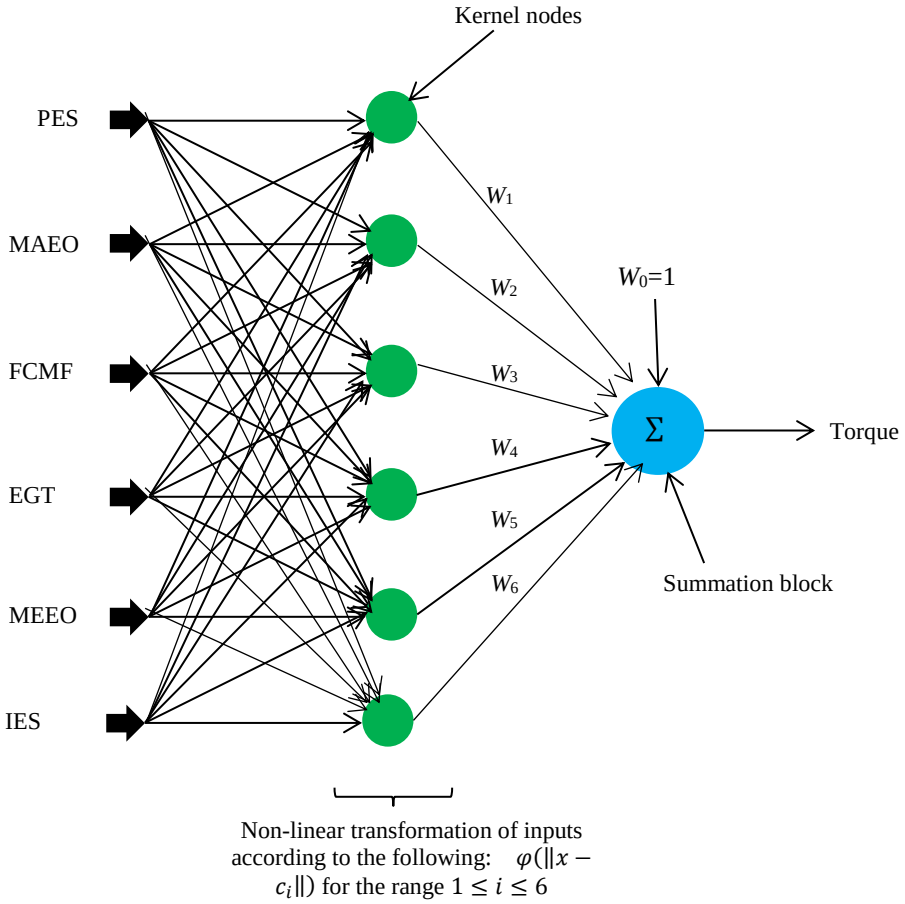

Figure 4. RBF feed-forward neural network.

Some important and common criteria including root mean squared error (RMSE), coefficient of determination (R^2), total sum of squared error (TSSE) and model efficiency (EF) were used to evaluate the models' performance. They are defined as follows [28]:

$$\text{RMSE} = \sqrt{\sum_{i=1}^{n} (dv - pv)^2 / n} \quad (2)$$

$$\text{R}^2 = \frac{\left(\sum_{i=1}^{n} \left(dv - \overline{dv}\right)(pv - \overline{pv})\right)^2}{\sum_{i=1}^{n} \left(dv - \overline{dv}\right)^2 \sum_{i=1}^{n} (pv - \overline{pv})^2} \quad (3)$$

$$\text{TSSE} = \sum_{i=1}^{n} (dv - pv)^2 \quad (4)$$

$$\mathrm{EF} = 1 - \frac{\sum_{i=1}^{n}(dv - pv)^2}{\sum_{i=1}^{n}(dv - \overline{pv})^2} \quad (5)$$

where *dv* is the actual (desired) output; *pv* is the predicted (fitted) output produced by the model; $\bar{d}$ and $\bar{p}$ are the average of the desired and predicted output, respectively. A model with the lowest RMSE and TSSE, and the highest EF and R^2 is considered to be the best.

The mean, variance, kurtosis and skewness of the actual and predicted datasets were statistically compared to evaluate the RBF model performance through the three phases of training, testing and total. Some statistical tests such as paired t-test, F-test and Kolmogorov–Smirnov test were used to compare the mean, variance and statistical distribution of the two datasets.

3. RESULTS AND DISCUSSION

Two parameters namely spread parameter and number of neurons in the hidden layer affect the performance prediction of RBF neural network. The variations of RMSE and EF for all data (train and test) versus spread parameter are shown in Figure 5 (a). The number of neurons in the hidden layer assumed to be constant and equal to 10. As it is seen, with increase in spread parameter, RMSE and EF had downward and upward trends, respectively. Our investigation showed that the trend of spread parameter variations changed for spread parameter of greater than 0.8. Figure 5 (b) shows the effect of number of neurons (hidden size) in the hidden layer on the performance of the RBF neural network. As shown in this figure, RMSE had downward trend with increase in the number of neurons. However, the number of neurons had no noticeable effect on EF. Hence, it can be concluded that EF is only affected by the optimum value of spread parameter. On the basis of Figure 5 it can be concluded that, having10 neurons is the best state for the network. Increasing the number of neurons more than 10, could lower the RMSE, however this reduction was negligible, considering training and computing times.

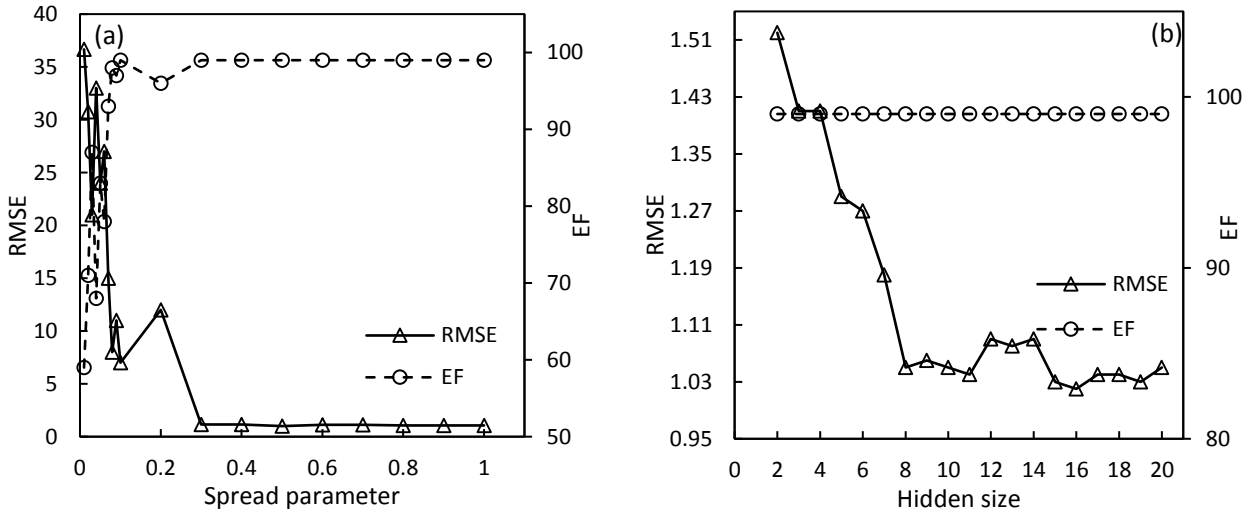

Figure 5. Variations of the RMSE and EF versus spread parameter and hidden size.

In the next step, the thirteen selected training algorithms mentioned in the materials and methods section were evaluated for engine torque predictions. The combination of completely randomized design (CRD) and k-fold cross validation methods was used to evaluate the training algorithms. The analysis of variance (ANOVA) of CRD is shown in Table 2 considering RMSE, TSSE, EF and R^2 criteria. Each training algorithm was trained using 20 different datasets obtained from 5-fold cross validation with four replications. Consequently, the total degree of freedom (df) of CRD was 259 according to the 13 treatments (training algorithms) and 20 replications (datasets). The p-values obtained from F statistic have demonstrated that the training algorithms have significant differences at the one percent of probability level based on the four performance criteria.

Means comparison of RMSE, TSSE, EF and R^2 criteria were performed using the LSD method. The means comparison result of performance criteria of 13 RBF's training algorithms is shown in Table 3. It is seen that RMSE and TSSE criteria have demonstrated the differences of the training algorithms better than R^2 and EF criteria, because most of the training algorithms except Traingdm have not significant differences with each other based on R^2 and EF criteria. Moreover, RMSE represents the differences of algorithms better than TSSE, because it classified the algorithms in various classes. Hence, the selection of algorithms was optimized based on

the smaller value of RMSE. The results showed that the Traindm algorithm, in comparison with the others, had the worst performance with significant difference at the one percent of probability level. The algorithms can be arranged based on RMSE in ascending order as follow: Trainbr, Trainbfg, Traincgb, Trainscg, Traincgf, Trainoss, Traincgp, Trainlm, Trainrp, Traingdx, Traingda, Traingdm and Traingda. Although the Trainlm algorithm has been used to train RBF in most of studies [27, 29], the results of the present study showed that this algorithm ranked eighth among the 13 algorithms and the Trainbr algorithm was selected as the best. It should be noted that although the Trainbr algorithm had no significant difference compared to the Trainbfg, its RMSE and TSSE values were 15 and 40 percent lower than the Trainbfg, respectively. The performance of RBF neural network might be varied with different data sets. Hence, among 20 different data sets from 5-fold cross validation, the data set was selected to lower the errors of training phase, assign good generalizability to the RBF network and prevent unfitness. Accordingly, the best training and test data sets were selected.

Table 2- ANOVA of the performance criteria of the RBF network for different training algorithms using CRD.

		RMSE		TSSE		EF		R^2	
Source	DF	SS	F-value	SS	F-value	SS	F-value	SS	F-value
Treatments[1]	12	4174.24	2654.83^{**}	50.37×10^{-9}	1019.6^{**}	0.1138	1019.96^{**}	0.0216	321.56^{**}
Errors	247	32.36		1.02×10^{-9}		0.0023		0.0014	
Total	259	4206.60		51.39×10^{-9}		0.1161		0.0230	

[1] The training algorithms; **significant at the 1 % level.

Table 3- Means comparison of the performance criteria of RBF network for various training algorithms.

Training algorithms	RMSE	TSSE	EF	R^2
Trainlm	1.14±0.23 cd	275.20±152.31 a	0.99±0.00 a	0.99±0.00 a
Trainbr	0.70±0.00 a	100.68±0.33 a	0.99±0.00 a	0.99±0.00 a
Trainscg	0.99±0.08 bcd	199.56±39.94 a	0.99±0.00 a	0.99±0.00 a
Trainrp	1.17±0.06 d	281.62±32.62 a	0.99±0.00 a	0.99±0.00 a
Traingdx	1.67±0.45 e	607.14±680.50 a	0.99±0.00 a	0.99±0.00 a
Traingdm	3.63±0.62 g	2753.68±956.54 b	0.99±0.00 b	0.99±0.00 b
Traingda	2.22±0.82 f	1137.91±1921.34 a	0.99±0.00 a	0.99±0.00 a
Traingd	15.53±1.65 h	49301.02±10256.70 c	0.92±0.01 c	0.96±0.01 a
Trainbfg	0.83±0.04 ab	140.20±16.24 a	0.99±0.00 a	0.99±0.00 a
Traincgb	0.94±0.07 bc	182.01±27.69 a	0.99±0.00 a	0.99±0.00 a
Traincgf	1.00±0.06 bcd	203.41±26.20 a	0.99±0.00 a	0.99±0.00 a
Traincgp	1.02±0.05 bcd	213.56±24.60 a	0.99±0.00 a	0.99±0.00 a
Trainoss	1.01±0.04 bcd	209.55±19.99 a	0.99±0.00 a	0.99±0.00 a

Means with the same letters are not significantly different.
The item with gray background shows the best training algorithm.

The result of RBF performance evaluation for estimating ITM285 tractor engine torque is shown in Table 4. As seen, the values of mean, variance, kurtosis and skewness of actual and predicted data sets in the training, test and total phases are displayed to evaluate the RBF model performance. As shown in this table, the differences between them are not considerable. Nevertheless, they were statistically compared together. Statistical tests namely paired t-test, F-test and Kolmogorov–Smirnov test were used to compare mean, variance and statistical distribution of the actual and predicted data sets, respectively. The p-values obtained from all tests were greater than 0.05. Consequently, both actual and predicted data sets did not have significant difference, statistically. Also, the values of RMSE and EF in the training and test phases were approximately equal (0.58). This shows that the RBF network has good generalizability.

Table 4- The RBF network performance for estimating engine torque.

	Train phase			Test phase			Total		
	Actual	Predicted	p-value	Actual	Predicted	p-value	Actual	Predicted	p-value
Average	86.23	86.23	0.99	98.33	98.33	0.99	90.15	90.15	0.99
Variance	3301.88	3300.81	0.99	2931.61	2930.07	0.99	3309.93	3309.06	0.99
Kurtosis	1.84	1.84	0.99	2.28	2.29	0.99	1.89	1.89	0.99
Skewness	0.17	0.17		0.35	0.35		0.15	0.15	
RMSE		0.59			0.58			0.58	
TSSE		56.39			13.22			69.70	
EF		0.99			0.99			0.99	

The agreement between the actual and predicted values during training and test phases is shown in Figure 6. As can be seen, the points are scattered around the line of 45 deg. On the other hand, the coefficient of determination (R^2) of regression line between the actual and predicted values was 0.99 in both training and test phases. Also, the slope and the intercept of the line are close to one and zero, respectively. Considering this

result, it can be concluded that there is a very good agreement between actual and predicted values in both training and test phases. Moreover, the agreement between actual and predicted values of torque for all samples during training and test phases is shown in Figure 7. Zweiri & Seneviratne [30] concluded that the average deviate between the measured and the estimated torque was not excessive and the nonlinear torque estimator based on ANN demonstrated a good agreement and high potential.

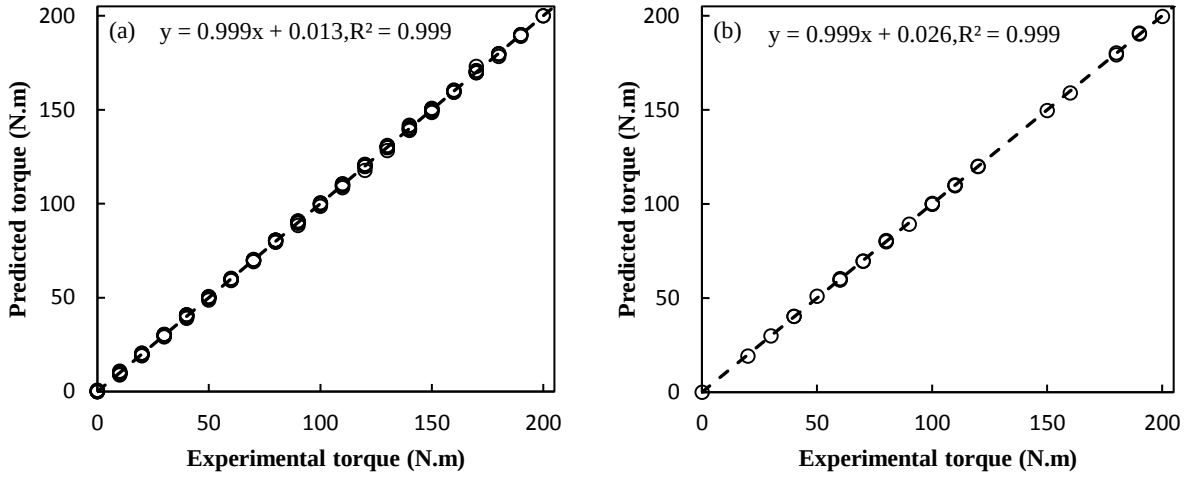

Figure 6. Scatter plot of the actual and predicted data sets in (a) training phase and (b) test phase.

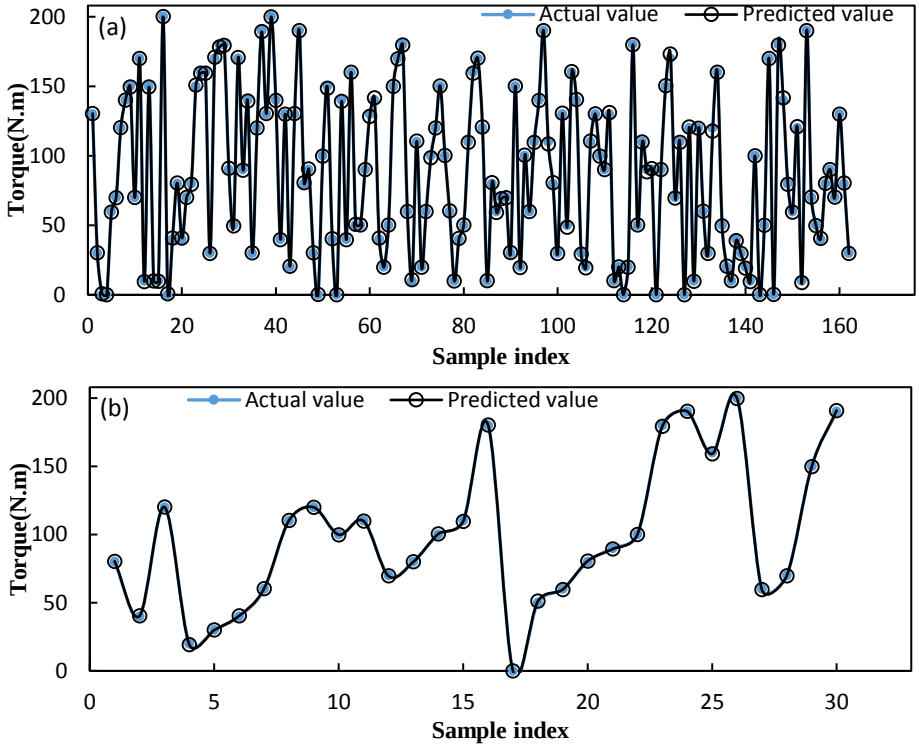

Figure 7. Actual and predicted values of torque in (a) training phase and (b) test phase, using RBF.

Sensitivity analysis was carried out to investigate the effect of the six studied variables for estimating engine torque. The sensitivity analysis results of the RBF model when excluding any of the input variables in training, test and total phases are shown in Table 5. As can be seen, the exclusion of four independent variables (PES, FCMF, EGT and IES) from the inputs of RBF neural network has increased the error (TSSE and RMSE) during the training, test and total phases. It is implied that for a better performance, this set of input variables of the network should be used; while the exclusion of the two remaining variables (MAEO and MEEO) can enhance the network performance. Consequently, the set of input variables including PES, FCMF, EGT and IES was used as the best combination. It can be concluded that using fore-mentioned variables and removing MAEO and MEEO can improve the network prediction performance. For instance, with this set of measurements the RMSE approximately decreased by 15 percent in training, test and total phases. Moreover, the unnecessary

measurement of the opacity parameter decreases estimation costs due to removal of the opacity sensor from measuring system of tractor engine torque. Franco et al. [12] mentioned that some variables such as pressure and temperature of intake and exhaust manifolds, engine speed, fuel quantity, and engine geometry have a significant impact on engine brake torque. In other research lubricant temperature was inappropriate (very low and diversified R^2) to model engine torque and BSFC using ANNs; while, EGT proved to be a suitable indirect estimator (R^2>0.993) [31].

Table 5- The sensitivity analysis results of the RBF model

Model	Input set	Train phase			Test phase			Total		
		RMSE	TSSE	EF	RMSE	TSSE	EF	RMSE	TSSE	EF
All	All	0.59	56.39	0.99	0.58	13.32	0.99	0.58	69.70	0.99
Sensitivity analysis	All exclude PES	0.69	77.55	0.99	0.68	19.02	0.99	0.69	96.57	0.99
	All exclude MAEO	**0.58**	**55.94**	**0.99**	**0.57**	**13.61**	**0.99**	**0.58**	**69.55**	**0.99**
	All exclude FCMF	0.72	85.79	0.99	0.72	21.22	0.99	0.72	107.01	0.99
	All exclude EGT	0.86	121.41	0.99	0.85	30.25	0.99	0.86	151.66	0.99
	All exclude MEEO	**0.59**	**57.28**	**0.99**	**0.58**	**14.22**	**0.99**	**0.59**	**71.53**	**0.99**
	All exclude IES	0.74	90.51	0.99	0.74	22.78	0.99	0.74	113.29	0.99
Proper selected input set	PES, FCMF, EGT, IES	0.50	40.90	0.99	0.51	10.60	0.99	0.50	51.49	0.99

4. CONCLUSIONS

With the aim of engine torque estimation, some models were developed based on ANNs, using some easy to measure working characteristics of ITM285 tractor including PES, IES, FCMF, EGT, MEEO and MAEO. Using the outcome of this research, the engine torque can be estimated using some low cost sensors instead of expensive devices and equipment (e.g. dynamometer). Sensitivity analysis demonstrated that two independent inputs of MAEO and MEEO can be eliminated from engine torque estimation procedure and better prediction performance can be gained by use of four inputs of PES, FCMF, EGT and IES.

The results of this research have shown that models based on soft computations are able to estimate the torque of ITM285 tractor's engine using data obtained from inexpensive and accessible sensors. Hence, the proposed models can be substituted with the conventional more expensive methods, using dynamometers.

5. ACKNOWLEDGMENT

The work presented in this paper is founded by Research Deputy of Ferdowsi University of Mashhad, Iran. It is part of a PhD thesis fulfilled in the Department of Biosystems Engineering. Their contributions are warmly acknowledged.

6. REFERENCES

1. Jones, N., and Li, Y.H. (2000), ‘‘A review of condition monitoring and fault diagnosis for diesel engines,’’ Lubrication Science, 6 (3), pp. 267-291, https://doi.org/10.1002/tt.3020060305.
2. Chamaillard, Y., Higelin, P., and Charlet, A. (2004), ‘‘A simple method for robust control design, application on a non-linear and delayed system: engine torque control,’’ Control Engineering Practice, 12 (4), pp. 417-429, https://doi.org/10.1016/S0967-0661(03)00113-8.
3. CK, I., MM, N., and CW, M.N. (2016), ‘‘Prediction of marine diesel engine performance by using artificial neural network Model,’’ Journal of Mechanical Engineering and Sciences (JMES), 10 (1), pp. 1917-1930, https://doi.org/10.15282/jmes.10.1.2016.15.0183.
4. Togun, N., Baysec, S., and Kara, T. (2012), ‘‘Nonlinear modeling and identification of a spark ignition engine torque,’’ Mechanical Systems and Signal Processing, 26, pp. 294-304, https://doi.org/10.1016/j.ymssp.2011.06.010.
5. Togun, N.K., and Baysec, S. (2010), ‘‘Prediction of torque and specific fuel consumption of a gasoline engine by using artificial neural networks,’’ Applied Energy, 87 (1), pp. 349-355, https://doi.org/10.1016/j.apenergy.2009.08.016.
6. Tosun, E., Aydin, K., and Bilgili, M. (2016), ‘‘Comparison of linear regression and artificial neural network model of a diesel engine fueled with biodiesel-alcohol mixtures,’’ Alexandria Engineering Journal, 55 (4), pp. 3081-3089, https://doi.org/10.1016/j.aej.2016.08.011.
7. Douglas, R., Steel, J., Reuben, R., and Fog, T. (2006), ‘‘On-line power estimation of large diesel engines using acoustic emission and instantaneous crankshaft angular velocity,’’ International Journal of Engine Research, 7 (5), pp. 399-410, https://doi.org/10.1243/14680874JER00206.
8. Lee, B., Rizzoni, G., Guezennec, Y., Soliman, A., Cavalletti, M., and Waters, J. (2001), ‘‘*Engine control using torque estimation,*’’ SAE Technical Paper, pp.
9. Lin, T.R., Tan, A.C., Ma, L., and Mathew, J. (2014), ‘‘*Estimating the loading condition of a diesel engine using instantaneous angular speed analysis*,’’ Springer, 259-272.

10. Rakotomamonjy, A., Le Riche, R., Gualandris, D., and Harchaoui, Z. (2008), ''A comparison of statistical learning approaches for engine torque estimation,'' Control Engineering Practice, 16 (1), pp. 43-55, https://doi.org/10.1016/j.conengprac.2007.03.009.
11. Ge, Y., Huang, Y., Hao, D., Li, G., and Li, H. (2016), ''An indicated torque estimation method based on the Elman neural network for a turbocharged diesel engine,'' Proceedings of the Institution of Mechanical Engineers, Part D: Journal of Automobile Engineering, 230 (10), pp. 1299-1313, https://doi.org/10.1177/0954407015606271.
12. Franco, J., Franchek, M.A., and Grigoriadis, K. (2008), ''Real-time brake torque estimation for internal combustion engines,'' Mechanical Systems and Signal Processing, 22 (2), pp. 338-361, https://doi.org/10.1016/j.ymssp.2007.08.002.
13. Shamekhi, A.-M., and Shamekhi, A.H. (2015), ''A new approach in improvement of mean value models for spark ignition engines using neural networks,'' Expert Systems with Applications, 42 (12), pp. 5192-5218, https://doi.org/10.1016/j.eswa.2015.02.031.
14. Tasdemir, S., Saritas, I., Ciniviz, M., and Allahverdi, N. (2011), ''Artificial neural network and fuzzy expert system comparison for prediction of performance and emission parameters on a gasoline engine,'' Expert Systems with Applications, 38 (11), pp. 13912-13923, https://doi.org/10.1016/j.eswa.2011.04.198.
15. Turkson, R.F., Yan, F., Ali, M.K.A., and Hu, J. (2016), ''Artificial neural network applications in the calibration of spark-ignition engines: An overview,'' Engineering Science and Technology, an International Journal, 19 (3), pp. 1346-1359, https://doi.org/10.1016/j.jestch.2016.03.003.
16. Ghotbi, M.R., Monazzam, M.R., Khanjani, N., Nadri, F., and Fard, S.M.B. (2013), ''Driver exposure and environmental noise emission of Massey Ferguson 285 tractor during operations with different engine speeds and gears,'' African Journal of Agricultural Research, 8 (8), pp. 652-659,
17. ASME (2012), ''*Reciprocating Internal-Combustion Engines*,'' Performance Test Codes (PTC 17), 17, pp. 1-33.
18. Canakci, M., Ozsezen, A.N., Arcaklioglu, E., and Erdil, A. (2009), ''Prediction of performance and exhaust emissions of a diesel engine fueled with biodiesel produced from waste frying palm oil,'' Expert Systems with Applications, 36 (5), pp. 9268-9280, https://doi.org/10.1016/j.eswa.2008.12.005.
19. OECD (2012), ''*OECD Standard Code for the Official Testing of Agricultural and Forestry Tractor Performance*,'' OECD Standard Codes (Code 2), pp. 1-91.
20. Sarvestani, N.S., Rohani, A., Farzad, A., and Aghkhani, M.H. (2016), ''Modeling of specific fuel consumption and emission parameters of compression ignition engine using nanofluid combustion experimental data,'' Fuel Processing Technology, 154, pp. 37-43, https://doi.org/10.1016/j.fuproc.2016.08.013.
21. Al-lwayzy, S.H., and Yusaf, T. (2017), ''Diesel engine performance and exhaust gas emissions using Microalgae Chlorella protothecoides biodiesel,'' Renewable Energy, 101, pp. 690-701, https://doi.org/10.1016/j.renene.2016.09.035.
22. Borgnakke, C., and Sonntag, R.E. (2012), ''*Fundamentals of Thermodynamics*,'' Wiley, New York, USA.
23. Manjunatha, R., Narayana, P.B., Reddy, K.H.C., and Reddy, K.V.K. (2012), ''Radial basis function neural networks in prediction and modeling of diesel engine emissions operated for biodiesel blends under varying operating conditions,'' Indian Journal of Science and Technology, 5 (3), pp. 2307-2312,
24. KÖKKÜLÜNK, G., AKDOĞAN, E., and Ayhan, V. (2013), ''Prediction of emissions and exhaust temperature for direct injection diesel engine with emulsified fuel using ANN,'' Turkish Journal of Electrical Engineering & Computer Sciences, 21 (Sup. 2), pp. 2141-2152, https://doi.org/10.3906/elk-1202-24.
25. Zhen-Tao, L., and Shao-mei, F. (2004), ''Study of CNG/diesel dual fuel engine's emissions by means of RBF neural network,'' Journal of Zhejiang University-SCIENCE A, 5 (8), pp. 960-965,
26. Wu, J.-D., Chiang, P.-H., Chang, Y.-W., and Shiao, Y.-j. (2008), ''An expert system for fault diagnosis in internal combustion engines using probability neural network,'' Expert Systems with Applications, 34 (4), pp. 2704-2713, https://doi.org/10.1016/j.eswa.2007.05.010.
27. Kumar, S., Pai, P.S., Rao, B.S., and Vijay, G. (2016), ''Prediction of performance and emission characteristics in a biodiesel engine using WCO ester: a comparative study of neural networks,'' Soft Computing, 20 (7), pp. 2665-2676, https://doi.org/10.1007/s00500-015-1666-9.
28. Rohani, A., Abbaspour-Fard, M.H., and Abdolahpour, S. (2011), ''Prediction of tractor repair and maintenance costs using artificial neural network,'' Expert Systems with Applications, 38 (7), pp. 8999-9007, https://doi.org/10.1016/j.eswa.2011.01.118.
29. Rezaei, J., Shahbakhti, M., Bahri, B., and Aziz, A.A. (2015), ''Performance prediction of HCCI engines with oxygenated fuels using artificial neural networks,'' Applied Energy, 138, pp. 460-473, https://doi.org/10.1016/j.apenergy.2014.10.088.
30. Zweiri, Y.H., and Seneviratne, D. (2007), ''*Diesel engine indicated torque estimation based on artificial neural networks*,'' Computer Systems and Applications, 2007. AICCSA'07. IEEE/ACS International Conference on, IEEE, pp. 791-798.
31. Bietresato, M., Calcante, A., and Mazzetto, F. (2015), ''A neural network approach for indirectly estimating farm tractors engine performances,'' Fuel, 143, pp. 144-154, https://doi.org/10.1016/j.fuel.2014.11.019.